4

FUZZY LOGIC CONTROLLERS FOR AIRCRAFT FLIGHT CONTROL

Jia Luo and Edward Lan

Department of Aerospace Engineering, University of Kansas
Lawrence, KA 66045, USA

ABSTRACT

Fuzzy logic proportional-integral-differential (PID) controllers are developed to perform both stability augmentation and automatic flight control functions. It operates for controlling both longitudinal and lateral- directional motions for an example aircraft, the X-29. The controllers for pitch, roll and yaw control are generated by analyzing a mathematical model describing aircraft static and dynamic characteristics. Each set of fuzzy rules consists of coarse and fine rules. The coarse rules are designed to supply fast response with large control input; while the fine rules are designed to make fine adjustments to improve dynamic stability. Nonlinear numerical simulations are performed to verify the controller performance at the design and off-design conditions for angle of attack hold, bank angle hold and sideslip angle hold. The results indicate that fuzzy PID controllers can provide fast, well damped response to pilot commands and thus improve flight performance, and increase agility, and also are robust.

1 INTRODUCTION

Fuzzy set was introduced by Zadeh to describe complex or ill-defined systems [1]. Soon after, it was applied to process control of systems for which the state variables could not be precisely measured [2]. Since then, fuzzy logic-based controllers have found many successful industrial applications and have demonstrated significant improvements in performance and robustness. However, they have not been utilized in flight control of operational aircraft in the past. Only recently has fuzzy logic been investigated for aerospace applications. For example, Larkin considered a fuzzy logic controller to control

an aircraft's final-approach flight path [3]. Chiu, et al. investigated active control of a flexible wing aircraft [4]. Application to helicopter design with multiple objectives has also been studied [5]. Application to space operations was discussed in [6]. However, the "fuzzy" concept has not been embraced by control engineers for high performance aircraft, such as fighters. It seems natural that fuzzy logic can be effectively implemented in a fighter control system since the aircraft characteristics have wide variation over a large flight envelope and some of these characteristics are not accurately known.

Flight control systems of high performance aircraft generally consist of two subsystems, one being the stability augmentation system (SAS) and the other being the automatic flight control system (AFCS)[7]. The former is to provide an aircraft with both statically and dynamically stable behaviors. The latter is mainly designed to avoid an unnecessary or dangerously high workload and to carry out all basic piloting functions. For the longitudinal motion, a typical SAS includes a pitch damper and a longitudinal stability SAS (α - SAS). The pitch damper is used to improve the short period handling quality by increasing damping, and the longitudinal stability SAS is to provide longitudinal static stability or stiffness. For the lateral-directional motion, a typical SAS consists of a yaw damper, a roll damper and a directional stability SAS (β -SAS). These are used to improve the Dutch-roll damping, decrease the roll mode time constant and increase the directional stiffness, respectively. Basic AFCS's have pitch attitude hold, altitude hold, bank angle hold, heading angle hold and other modes. Static and dynamic stabilities are very important properties an aircraft must possess. If the inherent stability is not available or not enough, stability augmentation should be employed in the flight control systems.

Agility is another important contributor to success in the modern air combat arena. A fighter aircraft with good longitudinal and lateral agility is capable of generating large instantaneous pitch, roll and yaw rates, without sacrificing controllability [8]. However, a fighter using a linear controller, even with gain scheduling, does not always have good agility. Large instantaneous pitch, roll or yaw rate may induce an unacceptable overshoot or total loss of controllability.

Fuzzy logic-based controllers for industrial applications are usually designed based on heuristic grounds to model a human operator's behavior. When a dynamic model describing a system's characteristics is available, albeit it is only approximate, it is advantageous to make use of such model to develop the fuzzy logic controller to create a truly robust control system [9]. In this chapter a fuzzy proportional-integral-differential (PID) flight control system

with some SAS and AFCS functions is developed for a sample aircraft, the X-29, to demonstrate this application. Fuzzy flight control system to provide fast, well damped responses to pilot pitch, yaw and roll commands will be presented.

2 FUZZY PID CONTROLLER

For a process described by linear mathematical models (transfer functions or state space equations), the linear proportional-integral-differential (PID) controllers can be employed to satisfy certain control specifications. In many engineering tasks, a linear model is obtained by linearizing a complicated nonlinear model at some operating condition to characterize the dynamics of the process. A PID controller designed based on this model is effective only in a small region around this operating condition. To describe the process dynamics quantitatively at other operating conditions, this model may not be precise enough. However, it may offer some qualitative information and physical insight, which can be used to develop a PID-like fuzzy controller. The objective is to develop a fuzzy controller which performs well in a wide range of conditions.

In the conventional linear control theory, the PID controller takes the form of

$$u = K_P(x - x_s) + K_I \int (x - x_s)dt + K_D \frac{dx}{dt} \tag{4.1}$$

where K_P, K_I and K_D are the proportional, integral and differential gains respectively. The integral part is included to drive x to its steady state, x_s, and the proportional and differential parts are used to modify the transient response of the closed loop system.

The incremental form for the PID controller, Eq. (4.1), from $t = (n-1)T$ to nT is

$$\begin{aligned} \Delta u(n) &= u(n) - u(n-1) \\ &= K_P\,[x(n) - x(n-1)] + (K_I T)\,[x(n) - x_s] + \\ &\quad (\frac{K_D}{T})\,[x(n) - 2x(n-1) + x(n-2)] \end{aligned} \tag{4.2}$$

$$\approx \quad (K_P T)\dot{x}(n) + (K_I T)\,[x(n) - x_s] + K_D T\ddot{x}(n)$$

Fuzzy PID controllers [10] have a similar structure to the linear PID controller and can be described in the following conditional statements:

If $\dot{x}$ is VP_j, $x - x_s$ is VI_j, and $\ddot{x}$ is VD_j,
then Δu is VU_j, $(j = 1, \ldots, n)$

where VP_j, VI_j, VD_j and VU_j represent suitable linguistic fuzzy values for the jth fuzzy rule.

The input of a fuzzy PID controller normally includes the first derivative of the state variable, $\dot{x}$, the error between the state variable and its set point, $x - x_s$, and the second derivative of the state variable, $\ddot{x}$. The controller output is the incremental control Δu. Given $\dot{x}$, $x - x_s$ and $\ddot{x}$, the value of Δu is generated through the fuzzification, fuzzy logic inference and defuzzification stages.

In the fuzzification stage, $\dot{x}$, $x - x_s$ and $\ddot{x}$ are scaled to the universe of discourse by suitable scaling factors G_p, G_i and G_d. The scaled variables or measurements are therefore

$$\bar{x_p} = Q\left[\frac{\dot{x}}{G_p}\right] \quad \bar{x_i} = Q\left[\frac{x - x_s}{G_i}\right] \quad \bar{x_d} = Q\left[\frac{\ddot{x}}{G_d}\right] \tag{4.3}$$

where Q represents quantifying a real number to its nearest integer.

In the fuzzy inference stage, by evaluating all n fuzzy rules in parallel the value of the degree of fulfillment of fuzzy incremental control at each point k on the universe of discourse is obtained as

$$\mu_U(k) = \max_{j=1}^{n} \{\min\left[VP_j(\bar{x_p}), VI_j(\bar{x_d}), VU_j(\nu_k)\right]\} \tag{4.4}$$

where ν_k represents the magnitude of the k^{th} point on the universe of discourse. The action taken in Eq. (4.4) can be interpreted as follows [9].

For given $\bar{x}_p, \bar{x}_i$ and $\bar{x}_d$, and at the k^{th} point for Δu, the degree of satisfaction or the compatibility of each fuzzy rule can be evaluated by the intersection or min-operation:

$$\omega_j = \min [VP_j(\bar{x}_p), VI_j(\bar{x}_i), VD_j(\bar{x}_d) VU_j(\nu_k)]$$

For example, VP_j may be positive medium, VI_j may be positive small, etc., and they are related by the connective operator AND so that the min-operation is needed. The degree of fulfillment involving all of these rules ($j = 1, \ldots, n$) is obtained by taking the union (or the max-operation) of the degrees of satisfaction of each rule. In other words, the rule that is most compatible with the values of $\bar{x}_p, \bar{x}_i, \bar{x}_d$, and ν_k is picked up for the k^{th} point:

$$\mu_U(\nu_k) = \max_{j=1}^{n} \omega_j$$

With the membership function, $\mu_U(\nu_k)$, the fuzzy incremental control can be converted into a deterministic control Δu by two possible defuzzification methods: the mean-of-maximum and the center-of-gravity procedures.

The mean-of-maximum procedure generates a value of Δu corresponding to the maximum grade of membership, $\mu_U(\nu_k)$. If there is more than one maximum value with the same magnitude, a value representing the mean of all local maxima is generated. This procedure does not consider the continuous variation in $\mu_U(\nu_k)$.

In the center-of-gravity procedure, the value of Δu representing the center of gravity of the membership function is generated. In this procedure the fuzzy incremental control at each point k on the universe of discourse has a contribution to Δu with a degree of $\mu_U(\nu_k)$ as follows:

$$\Delta u = G_u \frac{\sum_{k=1}^{m} \mu_U(\nu_k) \nu_k w_k}{\sum_{k=1}^{m} \mu_U(\nu_k)} \tag{4.5}$$

where G_u is the scaling factor for incremental control, ν_k represents the magnitude of the k^{th} point in the universe of discourse, and w_k is the weight

of the used fuzzy rule, which is employed to make further fine adjustments. In the present application, the center-of-gravity method will be used.

In the following a fuzzy PID flight control system is developed for the X-29 aircraft.

3 FUZZY FLIGHT CONTROL SYSTEM FOR THE X-29 AIRCRAFT

3.1 Conventional Stability Augmentation and Automatic Flight Control

To make an aircraft acceptable in flying qualities, certain levels of static and dynamic stability are required. Pitch, yaw and roll dampers are used to augment damping or dynamic stability by sensing angular rates and moving control surfaces to oppose the angular motion. To avoid serious divergence problems caused by a lack of inherent longitudinal or directional static stability, the α - SAS or β - SAS is employed to artificially increase the level of static stability or stiffness. Stability Augmentation Systems are normally in the inner loop of flight control systems. In the outer loop automatic flight control systems are employed to carry out certain tasks.

It should be noted that pitch control surface (elevator, or canard, symmetric and strake flaps for the X-29), yaw control surface (rudder), and roll control surface (aileron, or differential flap for the X-29) are functionally distinct in that the aileron is for the angular rate (p) control while the elevator and rudder are for the angular displacement (α or β) control. Therefore, from an analytical viewpoint, a PID angle of attack hold controller can be simply written as

$$\delta_c = KP_\alpha(\alpha - \alpha_s) + KI_\alpha \int (\alpha - \alpha_s)dt + KD_\alpha q \tag{4.6}$$

A PID sideslip hold controller can be represented by

$$\delta_r = KP_\beta(\beta - \beta_s) + KI_\beta \int (\beta - \beta_s)dt + KD_\beta r \tag{4.7}$$

and a PI bank angle hold controller can be

$$\begin{aligned} \delta_{df} &= KP_p(p - p_s) + KI_p \int (p - p_s)dt \\ &\approx KP_p(p - p_s) + KI_p(\phi - \phi_s) \end{aligned} \tag{4.8}$$

In the above equations, δ_c, δ_r and δ_{df} represent the deflections of canard, rudder and differential flap. For the X-29 aircraft, the other two longitudinal control surfaces, symmetric and aftbody strake flaps should have similar control functions to Eq. (4.6).

The differential parts in Eqs. (4.6) and (4.7), and the proportional part in Eq. (1.8) function as pitch, yaw and roll dampers and therefore improve dynamic stability. The proportional parts in Eqs. (4.6) and (4.7) are used to increase longitudinal and directional static stability, respectively. The integral parts in the above equations perform the outer loop tasks of command tracking.

In a digital flight control system the incremental forms of control functions shown in Eqs. (4.6), (4.7) and (4.8) can be implemented as follows:

$$\begin{aligned} \Delta\delta_c(n) &= KP_\alpha [\alpha(n) - \alpha(n-1)] + (KI_\alpha T)[\alpha(n) - \alpha_s] \\ &\quad + KD_\alpha [q(n) - q(n-1)] \\ &\approx (KP_\alpha T)\dot{\alpha}(n) + (KI_\alpha T)[\alpha(n) - \alpha_s] + (KD_\alpha T)\dot{q}(n) \end{aligned} \tag{4.9}$$

$$\begin{aligned} \Delta\delta_r(n) &= KP_\beta [\beta(n) - \beta(n-1)] + (KI_\beta T)[\beta(n) - \beta_s] \\ &\quad + KD_\beta [r(n) - r(n-1)] \\ &\approx (KP_\beta T)\dot{\beta}(n) + (KI_\beta T)[\beta(n) - \beta_s] + (KD_\beta T)\dot{r}(n) \end{aligned} \tag{4.10}$$

$$\begin{aligned} \Delta\delta_{df}(n) &= KP_p [p(n) - p(n-1)] + (KI_p T)[p(n) - p_s] \\ &\approx (KP_p T)\dot{p}(n) + (KI_p T)[p(n) - p_s] \end{aligned} \tag{4.11}$$

The above simplified PID control functions can be used for the analysis and development of corresponding fuzzy control rules and fuzzy control structure.

Variable	Unit	Trim Value
Altitude, h	ft	10,000
Mach Number, Mach		1.5
Angle of Attack,α	deg	0.86
Velocity, V	ft/sec	1616.0
Pitch Angle, θ	deg	0.86
Canard Deflection, δ_c	deg	0.59
Symmetric Flap, δ_{sf}	deg	-6.00
Strake Flap, δ_{st}	deg	-0.38
Throttle Position, δ_{th}		0.88

Table 1 Trim condition of the xxample aircraft.

3.2 Dynamic Characteristics Of The X-29 Aircraft

The X-29 aircraft has a forward-swept wing, and a high level of static instability (i.e. negative stiffness). The aircraft incorporates closed-coupled canards to provide a low-drag configuration. Longitudinal stability and control of the aircraft is obtained with canard, symmetric flap, and aftbody strake surfaces. Lateral-directional motion is controlled by the conventional rudder and differential flap deflection.

To develop a fuzzy logic based flight system for the X-29, the aircraft dynamic characteristics are examined first. From a nonlinear aerodynamic database, the X-29 linear model and trim condition can be generated [11]. In Table 1 a trim condition at a Mach number of 1.5 and h = 10,000 ft is listed,

and the locally linearized equations of motion are,

$$\begin{bmatrix} \dot{V} \\ \dot{\alpha} \\ \dot{q} \\ \dot{\theta} \end{bmatrix} = \begin{bmatrix} -0.07292 & 69.66020 & 0.00000 & -32.14209 \\ -0.00002 & -2.30449 & 1.00000 & 0.00000 \\ 0.00052 & 71.96335 & -3.56228 & 0.00000 \\ 0.00000 & 0.00000 & 1.00000 & 0.00000 \end{bmatrix} \begin{bmatrix} V \\ \alpha \\ q \\ \theta \end{bmatrix}$$

$$+\begin{bmatrix} -1.03806 & 1.10598 \\ -0.00088 & -0.00301 \\ 0.92282 & -0.58371 \\ 0.00000 & 0.00000 \end{bmatrix} \begin{bmatrix} \delta_c \\ \delta_{st} \end{bmatrix} \tag{4.12}$$

$$\begin{bmatrix} \dot{\beta} \\ \dot{p} \\ \dot{r} \\ \dot{\phi} \end{bmatrix} = \begin{bmatrix} -0.49268 & 0.01524 & -0.99988 & 0.01989 \\ -61.17613 & -7.83522 & 4.99085 & 0.00000 \\ 31.80377 & -0.23455 & -0.99414 & 0.00000 \\ 0.00000 & 1.00000 & -0.01524 & 0.00000 \end{bmatrix} \begin{bmatrix} \beta \\ p \\ r \\ \phi \end{bmatrix}$$
$$+\begin{bmatrix} -0.00197 & 0.00200 \\ 8.24620 & 1.84901 \\ 0.24926 & -0.43630 \\ 0.00000 & 0.00000 \end{bmatrix} \begin{bmatrix} \delta_{df} \\ \delta_r \end{bmatrix} \tag{4.13}$$

It should be noted that the state and control variables in the above linear equations are the perturbation variables from the trim conditions. From the above two equations it follows that the longitudinal static stability derivative is found to be

$$M_\alpha \approx 71.96 I_y > 0$$

which represents a high level of longitudinal static instability. The directional static stability derivative

$$N_\beta \approx 31.08 I_z > 0$$

however, indicates that directional static stability (or weathercock stability) is available. Because of the longitudinal static instability, no short period or phugoid mode exists, and any disturbance will cause divergence in the longitudinal motion.

The open-loop eigenvalues are listed in Table 2. The dynamic stability can be determined with the open-loop eigenvalues.

	Eigenvalues
Longitudinal	-11.4396, 5.5731, -0.0715, -0.0017
Lateral-Directional	-7.8164 (Roll), 0.0076 (Spiral), -0.7566±5.8062i (Dutch Roll)

Table 2 Open loop eigenvalues of the example aircraft.

Based on these stability analyses, an α - SAS and a pitch damper are required in the flight control systems to make the aircraft acceptable in flying qualities. However, excessive static stability can degrade overall performance. Since the directional static stability is inherently available, an β - SAS is not needed in the fuzzy flight control system; but a yaw damper is needed to increase dutch roll damping. The lateral- directional dynamic stability also needs to be improved. Optimal control theory can be applied to the above linear models to determine gains of the linear control functions given by Eqs. (4.6)-(4.8), which can be further used to generate the corresponding fuzzy control rules.

An integrator equation

$$\dot{\xi}_\alpha = \alpha - \alpha_s \tag{4.14}$$

will be added to Eq. (4.12) to find the control functions (Eq. 4.6) for the angle of attack hold. If the specified closed loop eigenvalues are -5.6±4.2i (short period), -0.25 and -0.015 (non-oscillatory phugoid), and -0.5 (integrator), then the resulting incremental control functions [12] can be obtained through a linear optimal control theory to be:

$$\begin{aligned} \Delta\delta_c \approx\ & [-(90.98T)\dot{\alpha} - (0.968T)(\alpha - \alpha_s) - (11.449T)\dot{q}] \\ & + (0.0416T)\dot{V} - (17.092T)\dot{\theta}, \end{aligned} \tag{4.15}$$

$$\Delta\delta_{st} \approx [(19.638T)\dot{\alpha} - (10.152T)(\alpha - \alpha_s) - (1.908T)\dot{q}]$$

$$- (0.007\ \mathrm{T})\ \dot{V} - (1.673T)\dot{\theta}.$$

For the lateral-directional motion, an integrator equation

$$\dot{\xi}_\beta = \beta - \beta_s \tag{4.16}$$

will be added to Eq. (4.13) to find the control functions (Eqs. 4.7 and 4.8). If the specified closed loop eigenvalues are -8.00 (roll), -0.05 (spiral), -4.883.66i (dutch roll), and -0.7 (integrator), then the resulting incremental control function 12 is determined, again by a linear optimal control theory, to be:

$$\begin{aligned} \Delta\delta_r \approx & \left[(3.41T)\dot{\beta} - (3.536T)(\beta - \beta_s) + (15.947T)\dot{r}\right] \\ & - (0.4126T)\dot{p} - (0.865T)(p - p_s) \end{aligned} \tag{4.17}$$

$$\begin{aligned} \Delta\delta_{df} \approx & \left[-(0.1576T)\dot{p} - (0.667T)(p - p_s)\right] \\ & + (1.01T)r - (0.8166T)\dot{r} + (0.2904T)(\beta - \beta_s) \end{aligned} \tag{4.18}$$

The sampling time T is taken to be 0.025 sec. It should be noted that in eqs. (4.15), (4.17) and (4.18) the terms included in the brackets have dominant roles in augmenting dynamic stability and keeping zero steady state errors. The relationships among fuzzy variables and the control structure in the fuzzy flight control system can be formulated based on these control functions.

3.3 Architecture Of Fuzzy Flight Control System

Fuzzy PID longitudinal and lateral-directional controllers for the X-29A Advanced Technology Demonstrator are set up and illustrated in Figs. 1 and 2.

Three sets of fuzzy control rules are generated for the angle of attack, sideslip angle and bank angle controls. These fuzzy PID control rules have similar structures to their conventional counterparts. The variables on the right hand side of Eqs. (4.6), (4.7) and (4.8) form the premises of fuzzy control rules, and the variables on the left hand side of these equations form the conclusions of the fuzzy control rules. In addition, fuzzy PID pitch attitude hold and heading

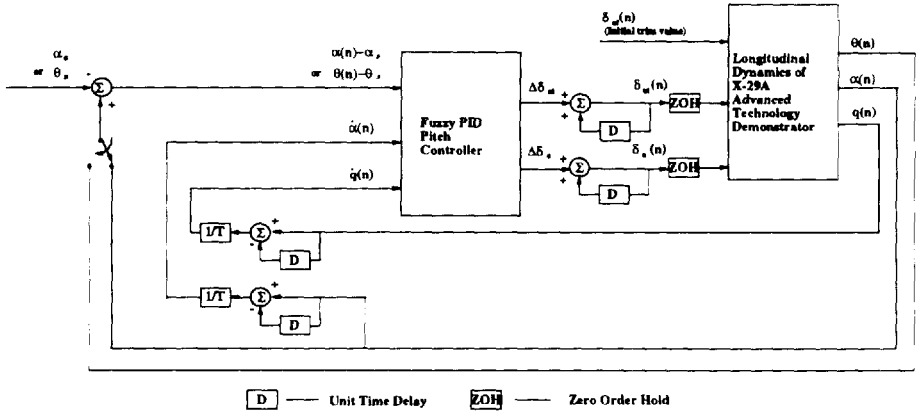

Figure 1 Block diagram of longitudinal fuzzy control for X-29.

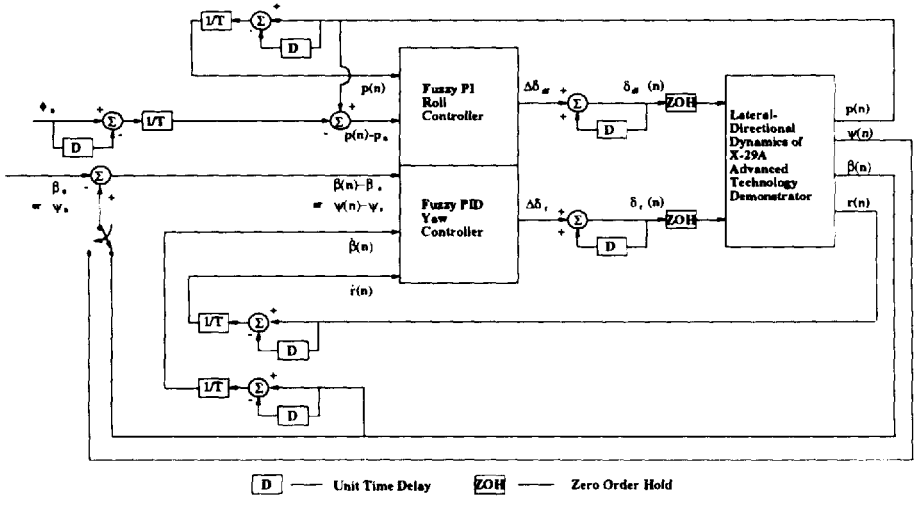

Figure 2 Block diagram of lateral-directional fuzzy control for X-29.

hold modes are also included in the present fuzzy flight control system. These fuzzy rules can be described by conditional statements as listed in Table 3.

Fuzzy PID α hold rules:	Fuzzy PID θ hold rules:
If $\alpha - \alpha_s$ is VI_j, $\dot{\alpha}$ is VP_j, and $\dot{q}$ is VD_j, then $\Delta\delta_c$ is VU_j, $\Delta\delta_{st}$ is VV_j, $(j = 1, \ldots, m_\alpha)$	If $\theta - \theta_s$ is VI_j, $\dot{\alpha}$ is VP_j, and $\dot{q}$ is VD_j, then $\Delta\delta_c$ is VU_j, $\Delta\delta_{st}$ is VV_j, $(j = 1, \ldots, m_\theta)$
Fuzzy PID β hold rules:	Fuzzy PID Ψ hold rules:
If $\beta - \beta_s$ is VI_j, $\dot{\beta}$ is VP_j, and $\dot{r}$ is VD_j, then $\Delta\delta_r$ is VU_j, $(j = 1, \ldots, m_\beta)$	If $\Psi - \Psi_s$ is VI_j, $\dot{\beta}$ is VP_j, and $\dot{r}$ is VD_j, then $\Delta\delta_r$ is VU_j, $(j = 1, \ldots, m_\Psi)$
Fuzzy PI ϕ hold rules:	
If $p - p_s$ is VI_j, and $\dot{p}$ is VP_j, then $\Delta\delta_{df}$ is VU_j, $(j = 1, \ldots, m_p)$	

Table 3 Forms of fuzzy control rules.

In the table VP_j, VI_j, VD_j and $VU_j (or VV_j)$ represent suitable linguistic fuzzy values for the j^{th} fuzzy control rule. These fuzzy values are chosen as: Negative Big(NB), Negative Medium(NM), Negative Small(NS), Around Zero(AZ), Positive Big(PB), Positive Medium(PM), Positive Small(PS). They are defined in the universe of discourse [-20, 20]. The corresponding membership functions are shown in Fig. 3.

3.4 Fuzzy Inference Rules

One of the most difficult and important problems in the design of fuzzy logic controllers is the generation of linguistic fuzzy control rules. Human operators' experience has played an important role in forming rules in many successful industrial applications. However, the empirical design approach is usually less efficient, time-consuming and even frustrating because some unclear, irrelevant and even incorrect information could be generated by human operators. For aircraft fuzzy controller design, the analysis of dynamic characteristics along with optimal control applications can make the generation of fuzzy rules more efficient, as will be presented in the following.

As described in the preceding section, the present fuzzy PID flight control system for the X-29 aircraft consists of three sets of rules to perform both stability augmentation and command tracking functions for pitch, yaw and

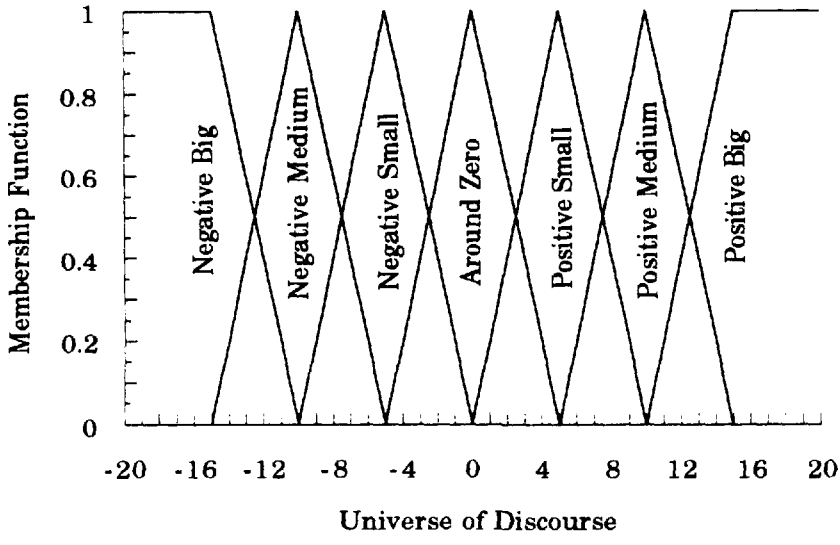

Figure 3 Membership functions.

roll motions. The number of fuzzy inference rules for each controller is basically determined by the combination of linguistic fuzzy values for each of premise variables in a fuzzy rule. For example, the pitch PID controller could have $7^3 = 343$ rules since all three premise variables, $\alpha - \alpha_s, \dot{\alpha}, \dot{q}$ as, , andq , are described by seven fuzzy values. Likewise, the yaw PID controller and the roll PI controller could have $7^3 = 343$ and $7^2 = 49$ rules, respectively. A large collection of fuzzy rules, however, may result in a relatively slow procedure for the fuzzy inference and evaluation, and thus makes the real-time implementation difficult. In the present fuzzy flight control system, the fuzzy inference rules are simplified by considering possible human operators' strategies which are quite different from those of linear PID controllers with constant gains. The present fuzzy control system includes coarse and fine rules generated for each set of rules [13]. The coarse rules are formed to use a large control action to quickly drive the controlled variables to set points or equilibrium points and also provide necessary static stability. Dynamic stability is augmented through the fine rules only when the variables come close to the set points or equilibrium points. The pitch, yaw and roll control rules for the X-29 are discussed below.

		$\dot{\alpha}$						
		NB	NM	NS	AZ	PS	PM	PB
$\alpha - \alpha_s$	NB	PB	PB	PB	PB	PB	PB	PS
	NM	PB	PB	PB	PB	PB	PS	NB
	NS	PB	PB	PB	PB	AZ	NB	NB
	AZ	PB	PB	PB		NB	NB	NB
	PS	PB	PB	AZ	NB	NB	NB	NB
	PM	PB	NS	NB	NB	NB	NB	NB
	PB	NS	NB	NB	NB	NB	NB	NB

Table 4 Coarse rules for a hold with canard (weight = 1) .

Pitch PID Control Rules

The X-29 aircraft has a high level of longitudinal instability as indicated earlier . Static stability should be provided with active canard, symmetric flap and aftbody strake flap. In the present study the deflection of the symmetric flap is kept at the initial trim value. Only canard and strake flap are employed in the fuzzy control. Referring to the linear PID control given by Eq. (4.15), the proportional gains (coefficients of $\dot{\alpha}$) are obviously larger than the integral and differential gains (coefficients of $\alpha - \alpha_s$ and $\dot{q}$). A small and positive $\dot{\alpha}$ could result in relatively large incremental changes of canard (negative) and strake flap (positive) to offer artificial static stability. Also, deviation of the angle of attack from its set point, $\alpha - \alpha_s$, has a minor contribution to the incremental changes of canard and strake flap. The fuzzy pitch control strategy can then be summarized as: as long as $\alpha - \alpha_s$ and $\dot{\alpha}$ are not close to zero, a larger control action should be taken to increase static stability and also quickly drive α to α_s with coarse rules no matter how large $\dot{q}$ is. When the angle of attack is close to the specified set point and $\dot{\alpha}$ is around zero, pitch damping is strongly imposed through fine rules to reduce oscillation around the set point. As a result, $7^2 - 1 = 48$ coarse rules are formed and listed in Tables 4 and 5 for both canard and strake flap control, respectively.

Notice that the upper left half of Table 4 and the lower right half of Table 5 represent for positive incremental changes in canard and strake flap, and the lower right half of Table 4 and upper left half of Table 5 represent negative incremental changes of these two control surfaces, respectively. The shaded areas include 7 fine rules which are listed in Tables 6 and 7.

		$\dot{\alpha}$						
		NB	NM	NS	AZ	PS	PM	PB
$\alpha - \alpha_s$	NB	NB	NB	NB	NB	NB	NB	PM
	NM	NB	NB	NB	NB	NB	PS	PB
	NS	NB	NB	NB	NB	AZ	PB	PB
	AZ	NB	NB	NB		PB	PB	PB
	PS	NB	NB	AZ	PB	PB	PB	PB
	PM	NB	NS	PB	PB	PB	PB	PB
	PB	NM	PB	PB	PB	PB	PB	PB

Table 5 Coarse rules for a hold with strake flap (weight = 1) .

For both $alpha - \alpha_s$ and $\dot{\alpha}$ are AZ,
if $\dot{q}$ is NB, then $\Delta\delta_c$ is PB,
else if $\dot{q}$ is NM, then $\Delta\delta_c$ is PM,
else if $\dot{q}$ is NS, then $\Delta\delta_c$ is PS,
else if $\dot{q}$ is AZ, then $\Delta\delta_c$ is AZ,
else if $\dot{q}$ is PS, then $\Delta\delta_c$ is NS,
else if $\dot{q}$ is PM, then $\Delta\delta_c$ is NM,
else if $\dot{q}$ is PB, then $\Delta\delta_c$ is NB.

Table 6 Fine rules for α hold with canard (weight < 1).

For both $alpha - \alpha_s$ and $\dot{\alpha}$ are AZ,
if $\dot{q}$ is NB, then $\Delta\delta_{st}$ is NB,
else if $\dot{q}$ is NM, then $\Delta\delta_{st}$ is NM,
else if $\dot{q}$ is NS, then $\Delta\delta_{st}$ is NS,
else if $\dot{q}$ is AZ, then $\Delta\delta_{st}$ is AZ,
else if $\dot{q}$ is PS, then $\Delta\delta_{st}$ is PS,
else if $\dot{q}$ is PM, then $\Delta\delta_{st}$ is PM,
else if $\dot{q}$ is PB, then $\Delta\delta_{st}$ is PB.

Table 7 Fine rules for α hold with strake flap (weight < 1) .

The fine rules are employed to reduce pitch oscillations only in regions around the set point α_s and therefore the values are reduced by weights being less than one, and actually function as a fuzzy pitch damper. The total number of coarse and fine rules for each control surface turns out to be $48 + 7 = 55$, which is much less than $7^3 = 343$. The selected 2×55 rules greatly speed up the process of fuzzy inference and evaluation.

For a small sideslip, the kinematic equation

$$\alpha \approx \theta - \theta_W \tag{4.19}$$

holds, where θ_W is the flight path angle. From Eq. (4.19) it follows that a positive $\Delta\theta$ normally corresponds to a positive $\Delta\alpha$. The fuzzy PID control rules for the angle of attack hold can be simply taken for the fuzzy pitch attitude hold with the premise variables $\alpha - \alpha_s$ replaced by $\theta - \theta_s$.

Yaw PID Control Rules

As far as the fuzzy yaw PID control is concerned , the fuzzy rules are supposed to take a similar form to the pitch control rules based on the same control strategy. The actual yaw control rules, however, are chosen slightly differently because of the particular directional dynamic characteristics. As analyzed in Section 3.2, the inherent directional static stability is available. Excessive static stability offered by a set of linguistic rules would degrade the performance and result in sluggish response. In the present yaw fuzzy controller the function performed by the proportional part (β) is simply removed from coarse rules. If the angular displacement error $\beta - \beta_s$ is not close to zero, the incremental change of rudder deflection is heavily dependent on the error regardless of the other variables. Therefore, a large and positive $\beta - \beta_s$ results in a large but negative $\Delta\delta_r$ based on the linear PID control given by Eq. (4.17), and so forth. When the sideslip is close to its set point β_s, the yaw rate may be very large due to the rapid decrease in $\beta - \beta_s$. The differential part ($\dot{r}$) will play an important role in reducing the yaw rate and also the roll rate caused by cross-coupling. Table 8 presents the coarse rules for yaw control.

In Table 8 the upper part represents the area for a positive rudder incremental change and the lower part is for a negative change. It should be noted that only 6 coarse rules are formed since the rudder incremental change

		$\dot{\beta}$						
		NB	NM	NS	AZ	PS	PM	PB
$\beta - \beta_s$	NB	PB	PB	PB	PB	PB	PB	PB
	NM	PM	PM	PM	PM	PM	PM	PM
	NS	PS	PS	PS	PS	PS	PS	PS
	AZ							
	PS	NS	NS	NS	NS	NS	NS	NS
	PM	NM	NM	NM	NM	NM	NM	NM
	PB	NB	NB	NB	NB	NB	NB	NB

Table 8 Coarse rules for β hold with rudder (weight = 1) .

For $\beta - \beta_s$ is AZ,
if $\dot{r}$ is NB, then $\Delta\delta_r$ is NB,
else if $\dot{r}$ is NM, then $\Delta\delta_r$ is NM,
else if $\dot{r}$ is NS, then $\Delta\delta_r$ is NS,
else if $\dot{r}$ is AZ, then $\Delta\delta_r$ is AZ,
else if $\dot{r}$ is PS, then $\Delta\delta_r$ is PS,
else if $\dot{r}$ is PM, then $\Delta\delta_r$ is PM,
else if $\dot{r}$ is PB, then $\Delta\delta_r$ is PB.

Table 9 Fine rules for β hold with rudder (weight < 1).

is independent of $\dot{\beta}$. In addition, the shaded area represents 7 fine rules which are listed in Table 9.

Similar to the pitch controller, the fine rules are used to reduce yaw oscillations only in regions around the set point β_s, and the control action is relatively small compared with that of the coarse rules. According to Eq. (4.17), this set of fine rules can be thought of as a fuzzy yaw damper. The total number of directional control rules is $6 + 7 = 13$, which is even smaller than that of pitch control rules.

At low angles of attack, the following kinematic equation holds according to the definition in flight dynamics,

$$\beta \approx \Psi_W - \Psi \tag{4.20}$$

Coarse Rules (Weight = 1)	Fine Rules (Weight ¡ 1)
if $p - p_s$ is NB, then $\Delta\delta_{df}$ is PB,	For $p - p_s$ is AZ,
else if $p - p_s$ is NM, then $\Delta\delta_{df}$ is PM,	if $\dot{p}$ is NB, then $\Delta\delta_{df}$ is PB,
else if $p - p_s$ is NS, then $\Delta\delta_{df}$ is PS,	else if $\dot{p}$ is NM, then $\Delta\delta_{df}$ is PM,
else if $p - p_s$ is PS, then $\Delta\delta_{df}$ is NS,	else if $\dot{p}$ is NS, then $\Delta\delta_{df}$ is PS,
else if $p - p_s$ is PM, then $\Delta\delta_{df}$ is NM,	else if $\dot{p}$ is AZ, then $\Delta\delta_{df}$ is AZ,
else if $p - p_s$ is PB, then $\Delta\delta_{df}$ is NB.	else if $\dot{p}$ is PS, then $\Delta\delta_{df}$ is NS,
	else if $\dot{p}$ is PM, then $\Delta\delta_{df}$ is NM,
	else if $\dot{p}$ is PB, then $\Delta\delta_{df}$ is NB.

Table 10 Roll PI control rules with differential flap.

in which Ψ_W is the azimuth angle of flight path. A positive $\Delta\Psi$ normally corresponds to a negative $\Delta\beta$. Accordingly the fuzzy PID rules for heading hold are similar to those for β hold except that the positive and negative areas of coarse rules in Table 8 are interchanged.

Roll PI Control Rules

The fuzzy PI roll control is intended to provide bank angle hold and also to improve dynamic lateral stability around the set point or the desired roll rate p_s through the differential flap . The fuzzy controller is also designed to model a human operator's strategy: No matter how large the roll acceleration $\dot{p}$ is, as long as the roll rate p is not close to its set point p_s, relatively large incremental changes in the differential flap should be used to quickly drive roll rate to its set point, the integral part being dominant. Once the roll rate comes close to its set points rapidly, the proportional part will play a more important role to impose damping and keep the roll rate p as close to p_s as possible with little or no oscillation. As a result, this fuzzy PI controller is highly nonlinear and time-varying. Based on the above control strategies and the linear control function given by Eq. (4.18), the roll control rules are formed and listed in Table 10.

The coarse rules correspond to the integral fuzzy roll control to reduce the roll rate error with relatively large incremental controls. Fine rules are employed to reduce or eliminate oscillations only in regions around the set point. Thus, incremental controls for the fine rules are weighted smaller than those used for the coarse rules.

From a dynamic point of view, the fine rule can be thought of as a fuzzy roll damper according to Eq. (4.18).

The fuzzy PID control algorithm described in Section 2 can now be adopted to compute the non-fuzzy control adjustments $\Delta\delta c, \Delta\delta st, \Delta\delta df$ and $\Delta\delta_r$ at each time step.

Care should be taken when choosing scaling factors because they have significant effects on the performance of the system being controlled. The determination of scaling factors used in the present application is discussed in following section.

3.5 Scaling Factors

The scaling factors have important effect on the system response [14]. They can take many possible values which can give just as good but probably not better response. The scaling factors of incremental control $\Delta\delta c, \Delta\delta st, \Delta\delta df$ and $\Delta\delta_r$ can be determined by using the given maximum deflection rates for each control surfaces. For the premise variables of control rules, the scaling factors are first estimated by evaluating possible large value of each variable, or using linear control gains. These estimated scaling factors are then adjusted to get better performance in terms of quick response and small tracking errors.

Firstly, the scaling factors of $\Delta\delta c, \Delta\delta st, \Delta\delta df$ and $\Delta\delta_r$ are determined based on an assumption that the maximum possible values of these incremental controls correspond to the maximum value on the universe of discourse, which is 20 in the present controller. For the X-29, the position and rate limits of deflection for these control surfaces are listed in Table 11 [15].

The scaling factors are then chosen as

$$
\begin{aligned}
G_c &= \tfrac{100T}{20}\,\text{deg} = \frac{100T}{20 \times 57.3} rad, \\
G_{st} &= \tfrac{30T}{20}\,\text{deg} = \frac{30T}{20 \times 57.3} rad, \\
G_{df} &= \tfrac{70T}{20}\,\text{deg} = \frac{70T}{20 \times 57.3} rad,
\end{aligned}
$$

Control surface	Position limit (deg)	Rate limit (deg/sec)
Canard	-60, 30	±100
Symmetric flap	-10, 25	±70
Strake flap	-30, 30	±30
Differential flap	-17.5, 17.5	±70
Rudder	-30, 30	±125

Table 11 Position and rate limits of control surfaces of the X-29.

$$G_r = \frac{100T}{20}\,\text{deg} = \frac{100T}{20 \times 57.3} rad,$$

where the sampling time T is taken to be 0.025 sec. In the linear control given by Eq. (4.18), the value of $p - p_s$ alone, corresponding to the maximum $\Delta\delta_{df}$, is $\frac{70T}{0.667T} = 105\,\text{deg}$. Therefore the initial estimate of the scaling factor for $p - p_s$ is $G_p = \frac{105}{20}\frac{\text{deg}}{sec} = \frac{105}{(20\times57.3)}\frac{rad}{sec}$. Similarly, the initial estimates of scaling factors for $\dot{p}$ is $G_{\dot{p}} = \frac{100T}{(57.3\times0.1567T)} = \frac{11}{20}\frac{rad}{sec^2}$. The initial estimates of G_p and $G_{\dot{p}}$ can also be found by evaluating $p_{\max}$ and $\dot{p}_{\max}$ from simulation or flight test data. Because the roll moment of inertia is much smaller than pitch and yaw moments of inertia, $\dot{q}_{\max}$ and $\dot{r}_{\max}$ are less than $\dot{p}_{\max}$. Hence, the estimates of $G_{\dot{q}}$ and $G_{\dot{r}}$ may be reduced to be less than $\frac{11}{20}\frac{rad}{sec^2}$. Also based on simulation and flight test data the reasonably large values for $|\alpha - \alpha_s|, |\beta - \beta_s|$ and $|\dot{\alpha}|$ can be set to $30\,\text{deg}, 30\,\text{deg}$ and $50\frac{\text{deg}}{sec}$, respectively. Their initial estimates could be $G_\alpha = G_{beta} = \frac{30}{20}$ deg, and $G_{\dot{\alpha}} = \frac{50}{20}\frac{deg}{sec}$. With the above estimates, extensive simulations are then made to update and modify these scaling factors to obtain good response to various commands. For this purpose, the scaling factors for each control system are systematically incremented from the initial estimates and tested for different types of command input (such as step, sinusoidal and ramp) and initial disturbances. The values giving response with small overshoots and tracking errors are those to be used. In the present fuzzy control system, the scaling factors for the angular acceleration are determined to be

$$G_{\dot{p}} = \frac{14}{20}\frac{rad}{sec^2}, \quad G_{\dot{q}} = \frac{6}{20}\frac{rad}{sec^2}, \quad G_{\dot{r}} = \frac{2}{20}\frac{rad}{sec^2}$$

and the scaling factor for $\dot{\alpha}$ is

$$G_{\dot{\alpha}} = \frac{40}{20}\frac{\text{deg}}{sec} = \frac{40}{20 \times 57.3}\frac{rad}{sec}$$

Slightly larger G_α, G_β and G_p offer better response to larger commands. In the present control system, they have been chosen as linear functions of $|\alpha - \alpha_s|, |\beta - \beta_s|$ and $|p - p_s|$, respectively to achieve better performance:

$$\begin{aligned}
G_\alpha(\alpha) &= \tfrac{25+0.5|\alpha-\alpha_s|}{20}\,\text{deg} &&= \frac{25 + 0.5|\alpha - \alpha_s|}{20 \times 57.3} rad \\
G_\beta(\beta) &= \tfrac{32+0.5|\beta-\beta_s|}{20}\,\text{deg} &&= \frac{32 + 0.5|\beta - \beta_s|}{20 \times 57.3} rad \\
G_p(p) &= \tfrac{30+2|p-p_s|}{20}\,\tfrac{\text{deg}}{sec} &&= \frac{30 + 2|p - p_s|}{20 \times 57.3}\frac{rad}{sec}
\end{aligned}$$

It should be pointed out that if the fuzzy control rules are generated based on dynamic analysis, the fuzzy controller performance is robust to a slight change of scaling factors.

For the pitch attitude and heading hold, the scaling factors of $\theta - \theta_s$ and $\Psi - \Psi_s$ can be simply chosen as

$$G_\theta(\theta) = G_\alpha(\theta), \quad G_\Psi(\Psi) = G_\beta(\Psi)$$

to provide good performance.

4 VALIDATION THROUGH NONLINEAR SIMULATION

To validate the fuzzy PID controllers developed above, nonlinear simulations are performed. The six degree-of-freedom nonlinear simulation program, SIMX29 [11] was modified by implementing the fuzzy PID control system. Nonlinear aerodynamic data from wing tunnel tests and thrust data are

incorporated in the simulation. A 4^{th} order Runge-Kutta scheme is used to numerically integrate the equations of motion. Also, a set of lateral-directional linear conventional PIF-CGT controllers [16] is compared with the present fuzzy controller in performance.

The deflection and rate limits of each control surfaces listed in Table 11 are used in the present nonlinear simulations. Aircraft tracking performance, stability, controllability and robustness with the fuzzy flight control system will be analyzed and discussed.

4.1 Fuzzy Pitch Control

To test the X-29 longitudinal performance with the fuzzy PID control system, closed loop response under angle of attack, pitch angle step commands, and initial disturbances are examined .

Figs. 4 and 5 present the time histories of angle of attack and pitch rate under a 10^o angle of attack step command. The corresponding deflection angles of canard and strake flap are given in Figs. 6 and 7. As shown in Fig. 4, the angle of attack can quickly reach the command value without overshoot. Canard and strake flap approach constant deflections to accomplish this maneuver.

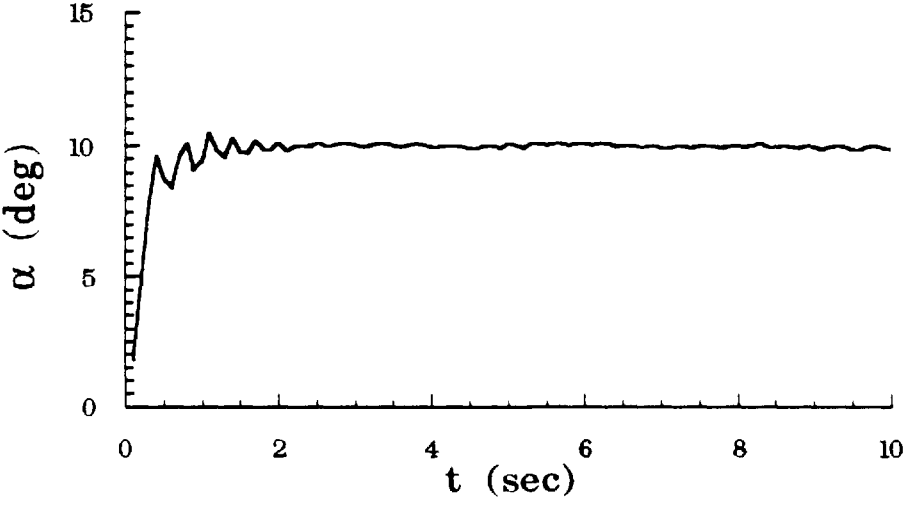

Figure 4 Angle of attack at step command $\alpha_s = 10^o$.

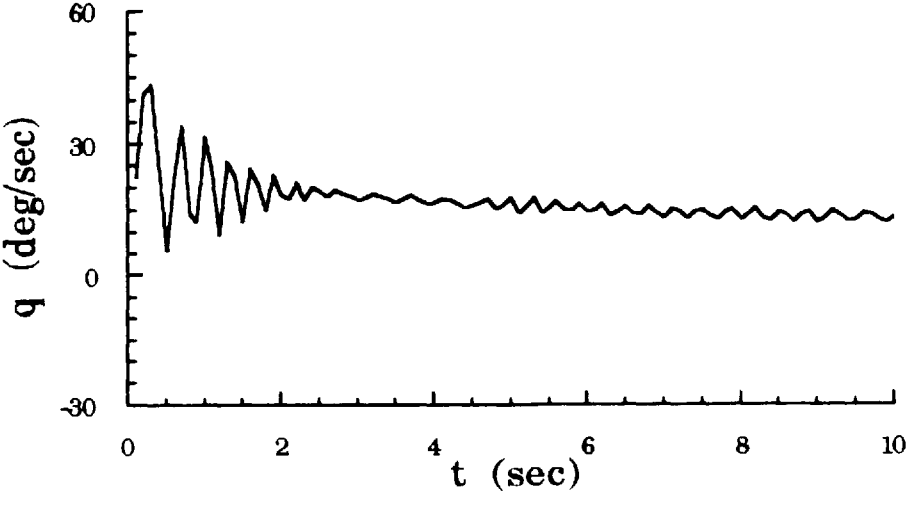

Figure 5 Pitch rate at step command $\alpha_s = 10^o$.

The same set of fuzzy control rules are employed to perform a 10^o pitch angle step command. The simulation results are given in Figs. 8 and 9. There is an

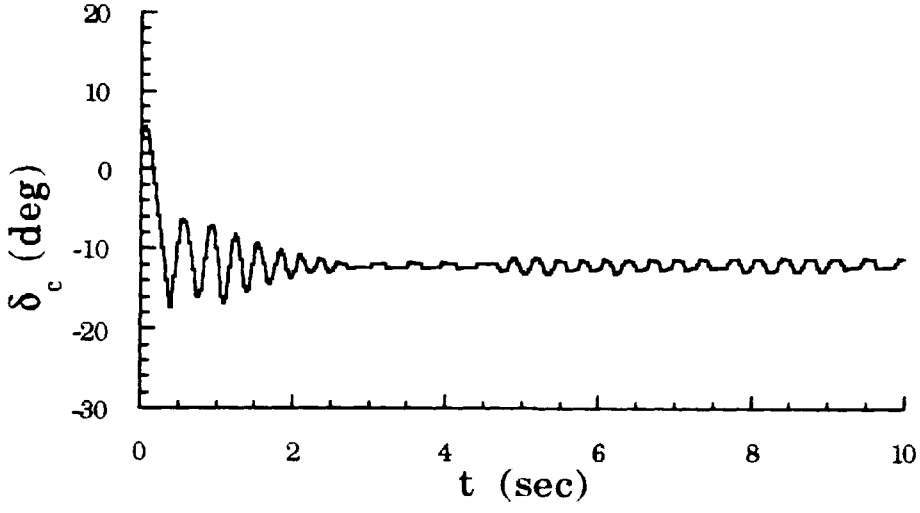

Figure 6 Canard deflection at $\alpha_s = 10°$.

overshoot in the pitch angle response as shown in Fig. 8. This is perhaps caused by using the same control rules as the α-hold indicated earlier. When the pitch angle reaches the commanded value $\theta_s = 10°$, the pitch rate is stabilized to zero. As a result, a new trim flight condition is reached through the fuzzy controller.

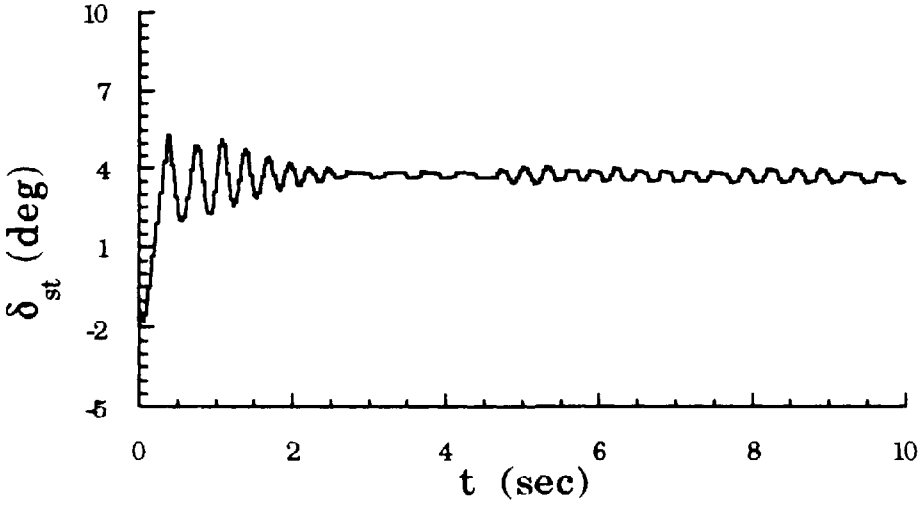

Figure 7 Strake flap deflection at $\alpha_s = 10^o$.

Fig. 10 shows the aircraft trajectories in the vertical plane at $\alpha_s = 10^o$ and $\theta_s = 10^o$. At the command of $\theta_s = 10^o$ the aircraft keeps a steady climb flight, while at the command of $\alpha_s = 10^o$ the aircraft makes a loop maneuver.

In Figs. 11 and 12, responses of angle of attack and pitch rate at a command of $\alpha_s = 15^o$ (an off- design condition) are given. The well-behaved responses illustrate the robustness of the fuzzy controller.

4.2 Fuzzy Yaw Control

The directional fuzzy PID controller is developed to perform yaw dynamic stability augmentation and automatic flight control functions such as sideslip hold and heading hold. This fuzzy controller can be evaluated by examining the aircraft response to step commands of sideslip and heading angle, and initial disturbances. Some of the responses by the fuzzy controller are also compared with those by a linear PIF-CGT controller .

Figures 13 and 14 present the time histories of sideslip angle and yaw rate under a 10^o sideslip step command. The sideslip response with a rise time of

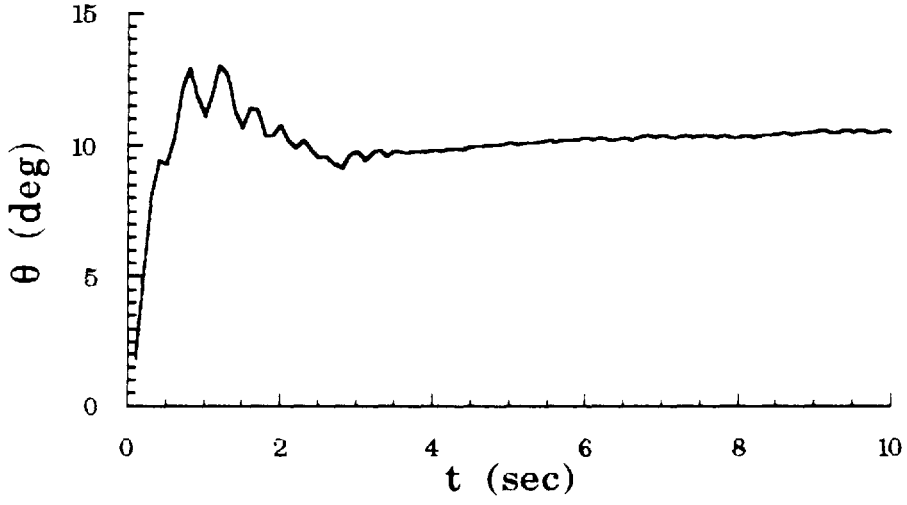

Figure 8 Pitch angle at step command $\theta_s = 10°$.

0.55 sec by the fuzzy controller was much faster than that with a rise time of 2.10 sec by a linear controller in Fig. 13. The yaw rate generated by the fuzzy controller was larger compared with that of the linear controller as shown in Fig. 14. Short transition times and engagement which are needed by modern fighter aircraft can be obtained with the fuzzy controller, and thus good yaw agility can be achieved. The corresponding deflection angles and rates of differential flap and rudder are given in Figs. 15 and 16. Control of this maneuver mainly comes from the rudder deflection. The differential flap deflection also makes a small contribution to this maneuver in addition to keeping the roll rate close to zero at a steady state sideslip.

The responses of heading angle and yaw rate to a heading step command of $\Psi = 10^o$ are shown in Figs. 17 and 18. With the fuzzy yaw PID controller, the heading angle is quickly driven to the command value. The yaw rate is also quickly damped to zero with the fine rules in the fuzzy controller. Consequently, the aircraft is switched to a new trim condition that is the same as the initial flight condition except the change in heading angle.

Figure 19 shows the aircraft trajectories in the horizontal plane at $\beta_s = 10^o$ and $\Psi_s = 10^o$. At the command of $\Psi_s = 10^o$ the aircraft keeps a straight and

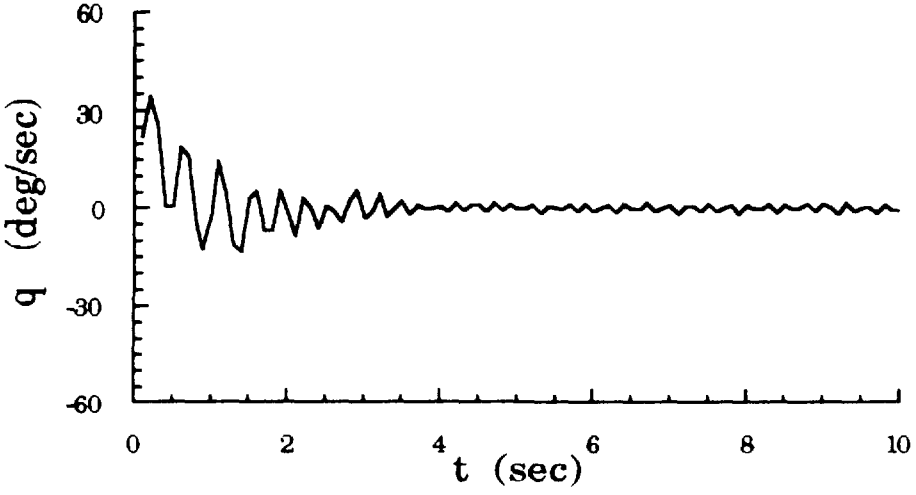

Figure 9 Pitch rate at step command $\theta_s = 10^o$.

level flight with a heading angle of 10^o, while at the command of $\beta_s = 10^o$ the aircraft makes a slight left turn with a 10^o sideslip and zero bank angle.

In Figures 20 and 21, under a 15^o sideslip step command (an off-design condition), the fuzzy controller still performed well, but the linear controller lost the controllability of both surfaces with divergent sideslip and yaw rate as a result.

4.3 Fuzzy Roll Control

The X-29 roll performance with the fuzzy flight control system is tested through bank-to-bank maneuvers . Figs. 22 and 23 show the time histories of bank angle and roll rate during a 40^o bank-to-bank maneuver. In Fig. 22 the bank angle response by the fuzzy controller is shown to almost exactly follow the command, but the response of the linear PIF-CGT controller has large overshoots at turning points. The roll rate by the fuzzy controller is much faster than that of the linear controller as shown in Fig. 23. This indicates that the fuzzy controller can significantly improve the roll performance and

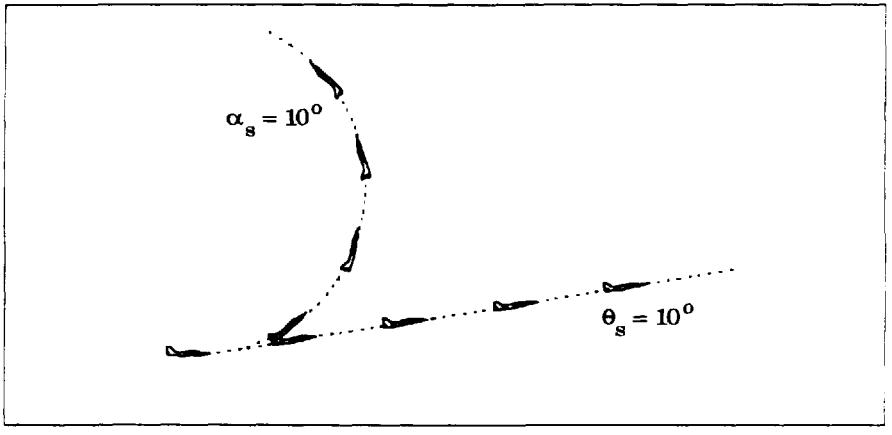

Figure 10 Trajectory in vertical plane for $\alpha_s = 10^o$ hold and $\theta_s = 10^o$.

increase its agility. Control surface deflections of differential flap and rudder in Figs. 24-25 are within their limits. This maneuver is accomplished mainly by the differential flap control as shown in Fig. 24. Rudder deflection is mainly used to reduce sideslip excursion during the bank-to-bank maneuver.

In Figure 26, the bank angle responses by the same fuzzy controller and a linear controller during a 70° bank-to-bank maneuver are given. An excellent response is obtained by the fuzzy controller, but the linear controller generates a divergent response. The roll rate response by the fuzzy controller during this maneuver has slight overshoots but is damped quickly to the commanded value while the linear controller induces an unacceptable roll rate response as shown in Fig. 27.

For additional simulation results, readers should consult Reference 12.

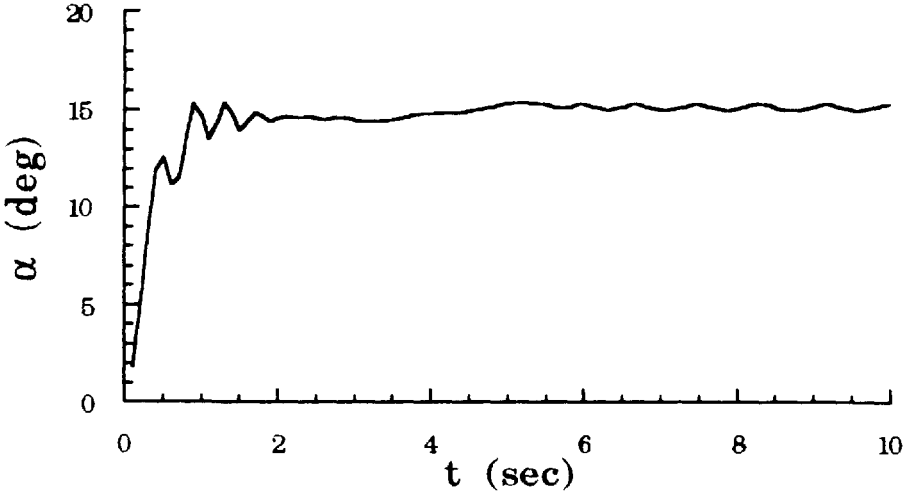

Figure 11 Angle of attack at step command $\alpha_s = 15^o$.

5 CONCLUSIONS

Fuzzy logic technology has been applied to flight control to enhance aircraft performance. The design procedure of a fuzzy flight control system was studied and presented with a sample aircraft, the X- 29. Through nonlinear simulations of the system performance, it could be concluded that:

1. A pure fuzzy logic controller could perform both stability augmentation and automatic flight control functions with coarse and fine control rules.
2. A fuzzy flight control system could be developed based on aircraft dynamic analysis and optimal control of a linearized model along with possible human operators' strategy.
3. Aircraft with a fuzzy control system behaved nonlinearly even with a linear open loop system. A fuzzy controller could offer excellent performance in terms of quick response and small tracking errors to achieve highly nonlinear control objectives.

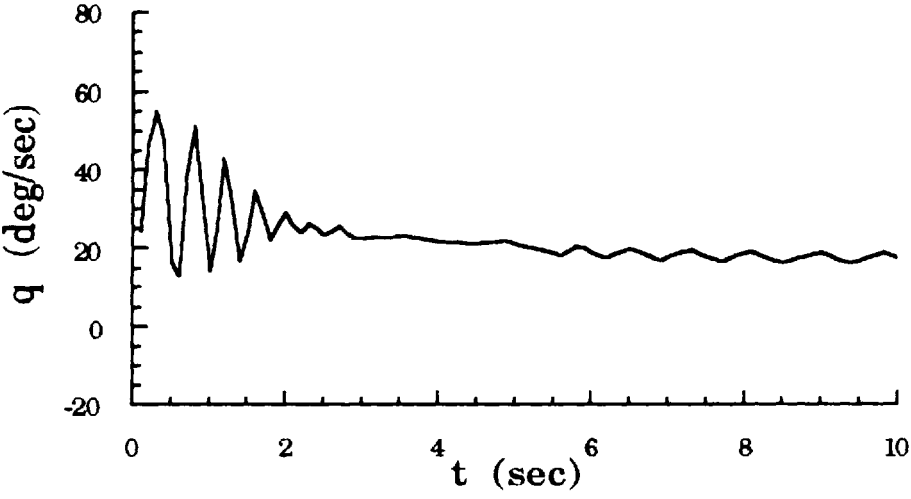

Figure 12 Pitch rate at step command $\alpha_s = 15°$.

4. A fuzzy flight control system was capable of utilizing the potential of control surfaces to generate large angular rates without sacrificing controllability, and thus to greatly improve aircraft agility.

5. A fuzzy flight control system was robust compared with a conventional control because all the control rules were evaluated for an existing flight condition before any control action was taken.

REFERENCES

[1] Zadeh, L. A., "Outline of a New Approach to the Analysis of Complex Systems and Decision Processes," IEEE Trans. Syst., Man, Cybern., Vol. SMC-3, No. 1, pp. 28-44, 1973.

[2] Mamdani, E. H. and Assilian, S., "An Experiment in Linguistic Synthesis with a Fuzzy Logic Controller," Int. J. Man-Machine Studies, Vol. 7, pp. 1-13, 1975.

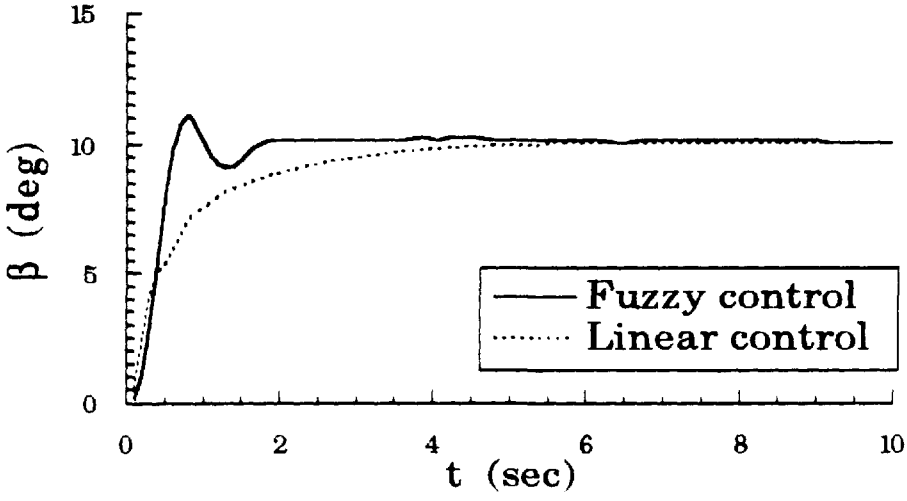

Figure 13 Sideslip angle at step command $\beta_s = 10°$.

[3] Larkin, L. I., "A Fuzzy Logic Controller for Aircraft Flight Control," Industrial Applications of Fuzzy Control, edited by M. Sugeno, Elsevier Science Publishers B. V. (North-Holland), 1985.

[4] Chiu, S., Chand, S., Moore, D., and Chaudhary, A., "Fuzzy Logic for Control of Roll and Moment for a Flexible Wing Aircraft," IEEE Control Systems Magazine, June 1991, pp.42-48.

[5] Rao, S. S. and Dhingra, A. K., "Applications of Fuzzy Theories to Multi-Objective System Optimization," NASA CR-177573, Jan. 1991.

[6] Villarreal, J. A.; Lea, R. N.; and Savely, R. T., "Fuzzy Logic and Neural Network Technologies," AIAA Paper 92-0868, Jan. 1992.

[7] Roskam, J., Airplane Flight Dynamics and Automatic Flight Controls, Part II, Roskam Aviation and Engineering Corporation, Ottawa, KS, 1982.

[8] Valasek, J., Eggold, D., and Downing, D., "A Study of a Proposed Modified Torsional Agility Metric," AIAA Paper 91-2883-CP, August 1991.

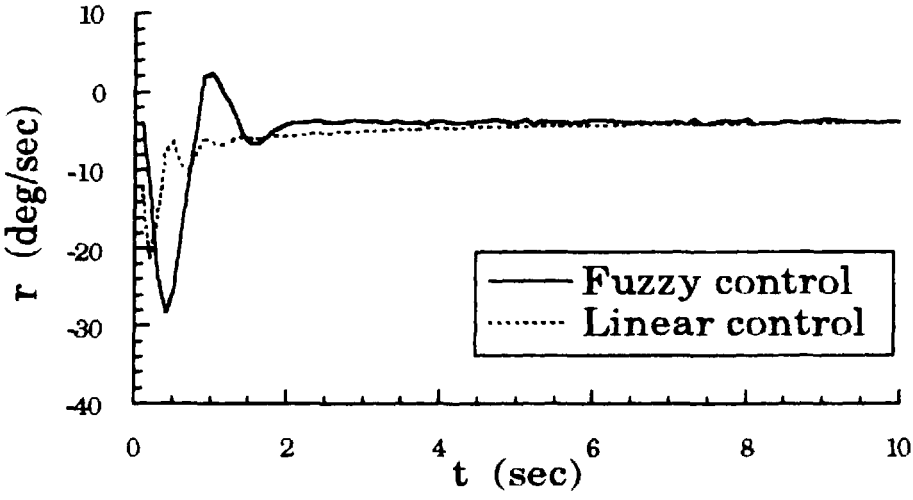

Figure 14 Yaw rate at step command $\beta_s = 10^o$.

[9] Bernard, J. A., "Use of a Rule-Based System for Process Control," IEEE Control Systems Magazine, Oct. 1988, p.3.

[10] Peng, X., Liu, S., Yamakawa, T., Wang, P., and Liu, X., "Self-regulating PID Controller and its Applications to a Temperature Controlling Process," Fuzzy Computing-Theory, Hardware, and Applications, edited by Gupta, M., and Yamakawa, T., Elsevier Science Publishers, 1988, pp.355- 364.

[11] Linse, D., "Design and Analysis of a High Angle of Attack Flight Controls System," MS thesis, the University of Kansas, 1987.

[12] Luo, J., "Aircraft Control Based on Fuzzy Logic," Ph.D Dissertation, the University of Kansas, 1994.

[13] Luo, J., and Lan, C. Edward, "Development and Performance of a Fuzzy Logic Lateral Controller for X-29 Aircraft," International Fuzzy Systems and Intelligent Control Conference, March 1993, Louisville, KY.

[14] Procyk, T., and Mamdani, E., "A Linguistic Self-Organizing Process Controller," Automatica, Vol. 15, 1979, pp. 15-30.

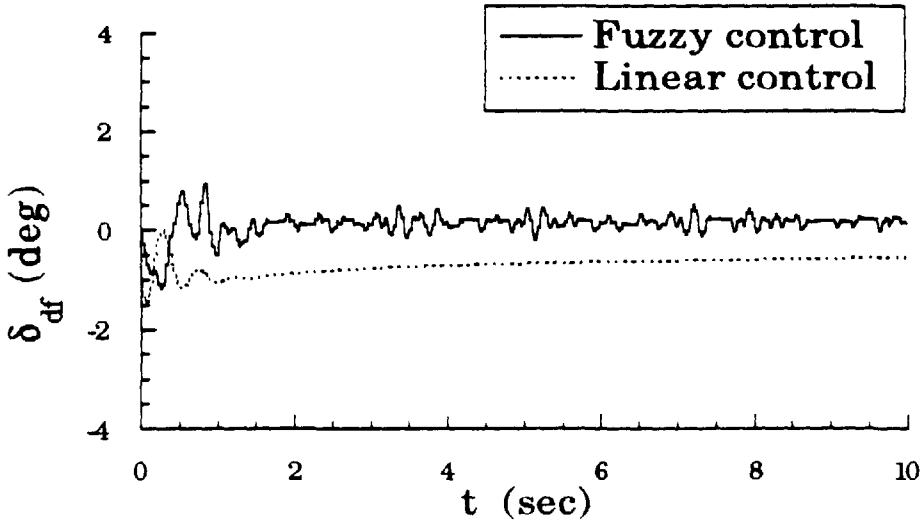

Figure 15 Differential flap deflection at step command $\beta_s = 10°$.

[15] Bosworth, John T., "Linearized Aerodynamic and Control Law Models of the X-29A airplane and Comparison with Flight Data," NASA Technical Memorandum 4356, February 1992.

[16] Suikat, R., "An Optimal Pole Placement Gain Scheduling Algorithm Using Output Feedback," Ph.D Dissertation, the University of Kansas, 1987.

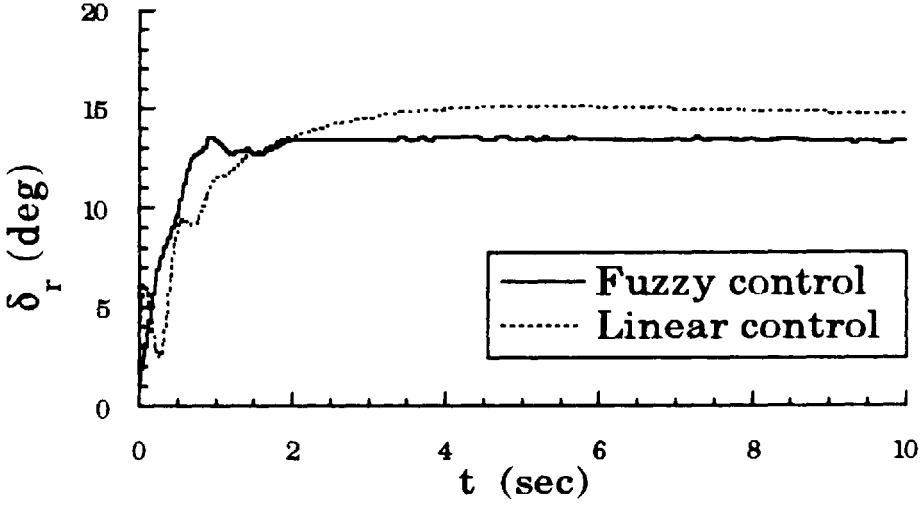

Figure 16 Rudder deflection at step command $\beta_s = 10°$.

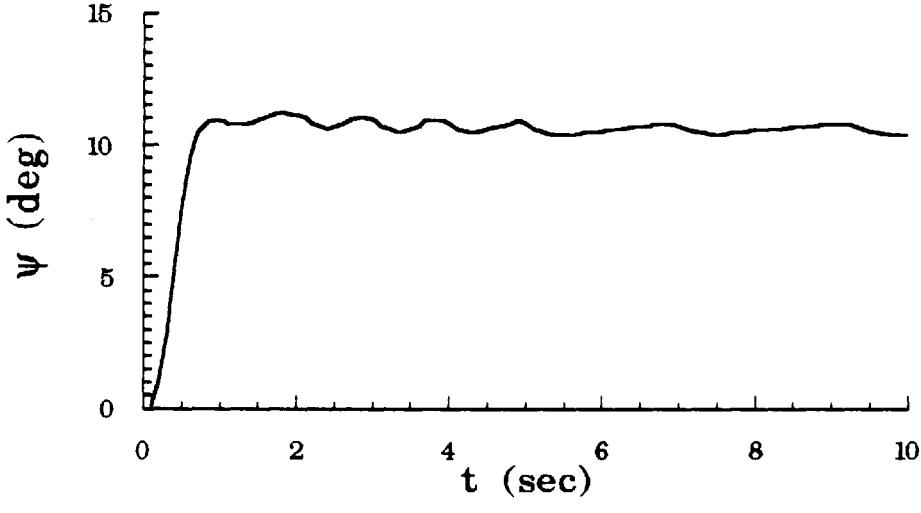

Figure 17 Heading angle at step command $\Psi_s = 10°$.

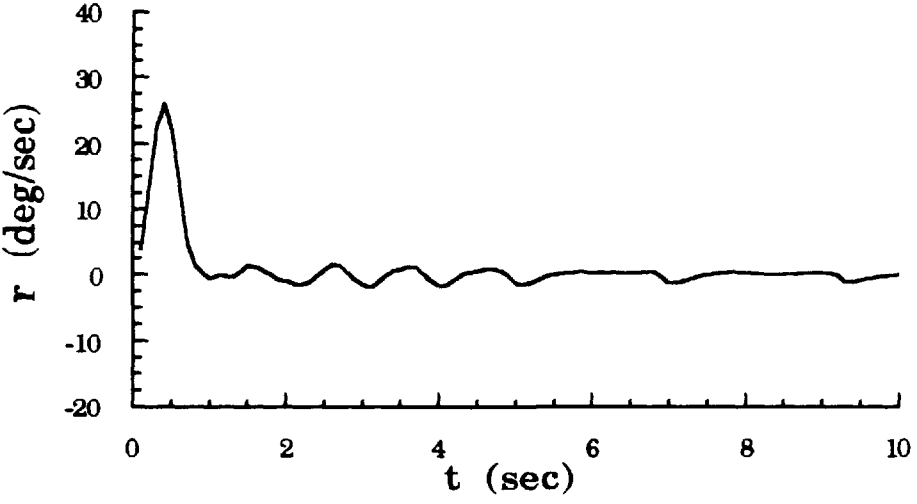

Figure 18 Yaw rate at step command $\Psi_s = 10^o$.

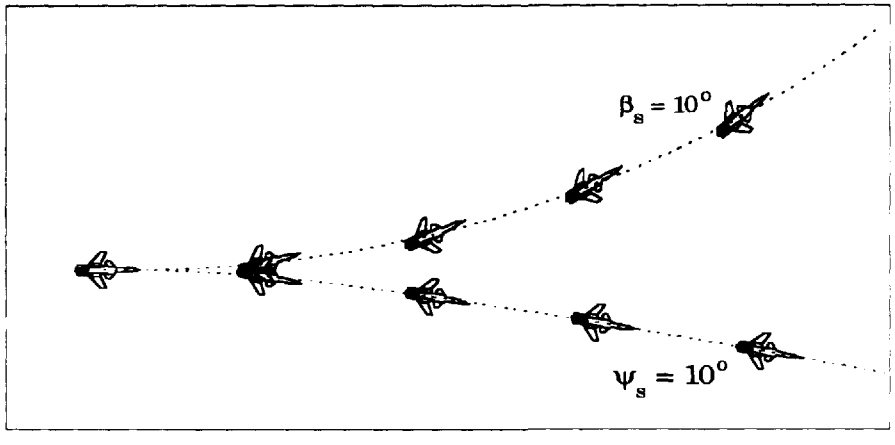

Figure 19 Trajectories in horizontal plane for $\beta_s = 10^o$ hold and $\Psi_s = 10^o$.

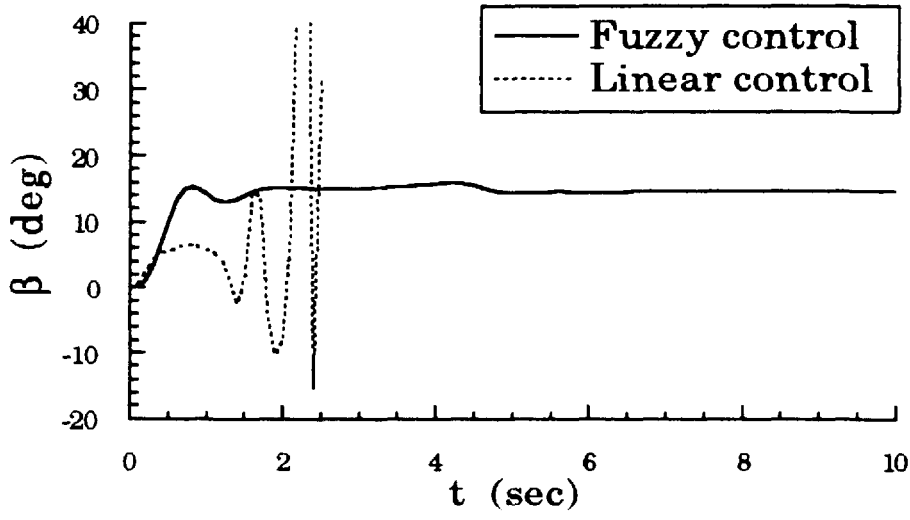

Figure 20 Sideslip angle at step command $\beta_s = 15°$.

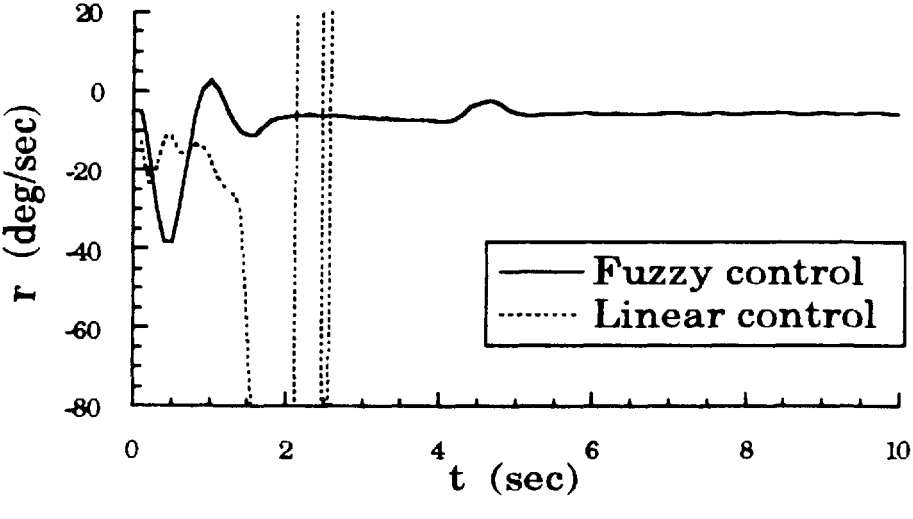

Figure 21 Yaw rate at step command $\beta_s = 15°$.

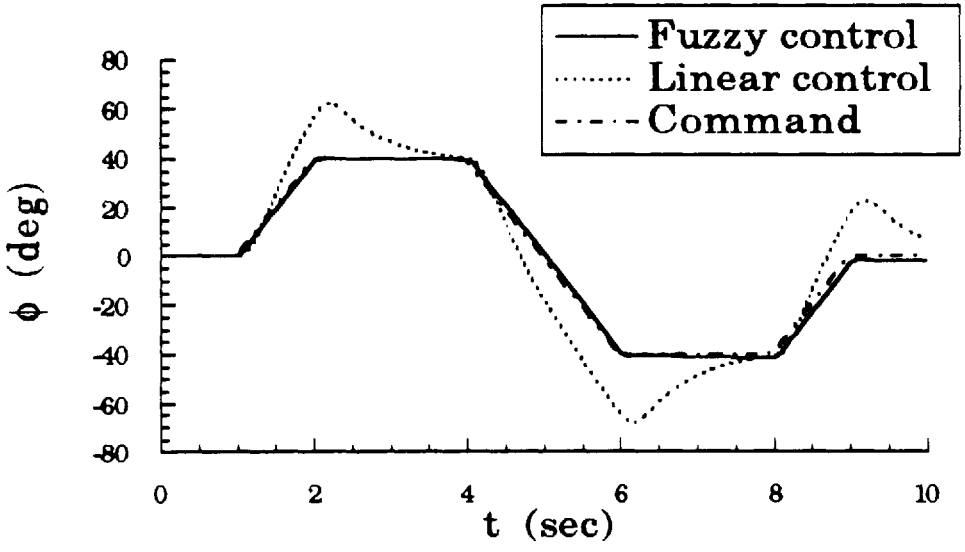

Figure 22 Bank angle at a 40° bank-to-bank command.

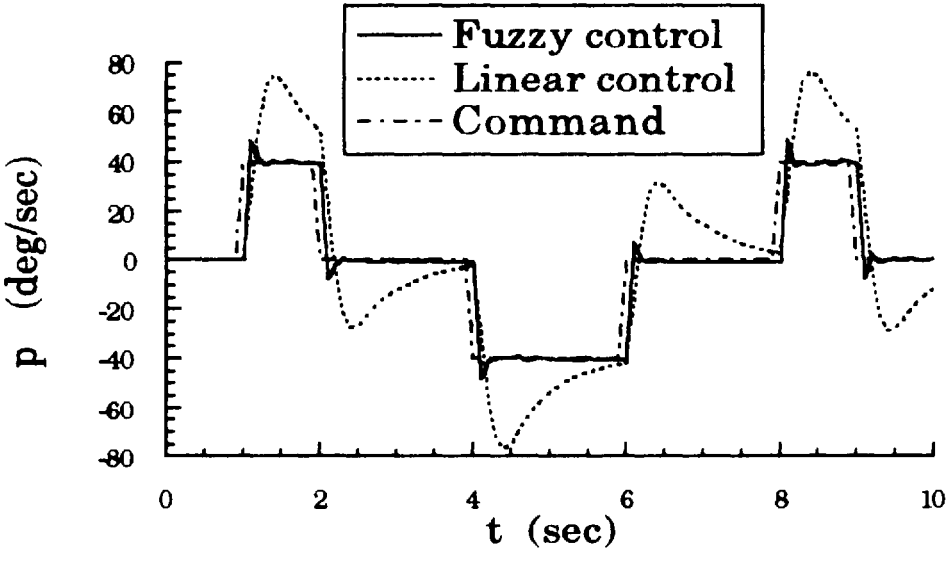

Figure 23 Roll rate at a 40° bank-to-bank command.

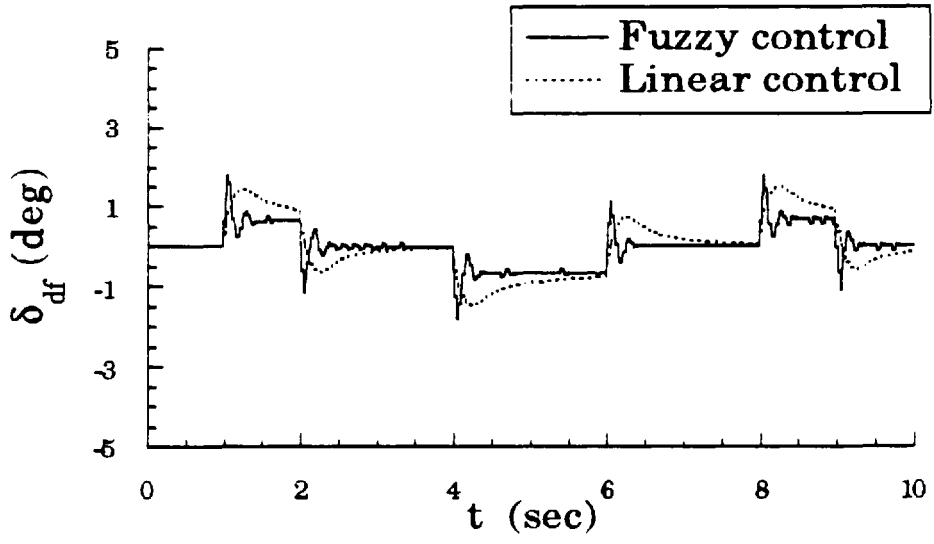

Figure 24 Differential flap deflection at a 40° bank-to-bank command.

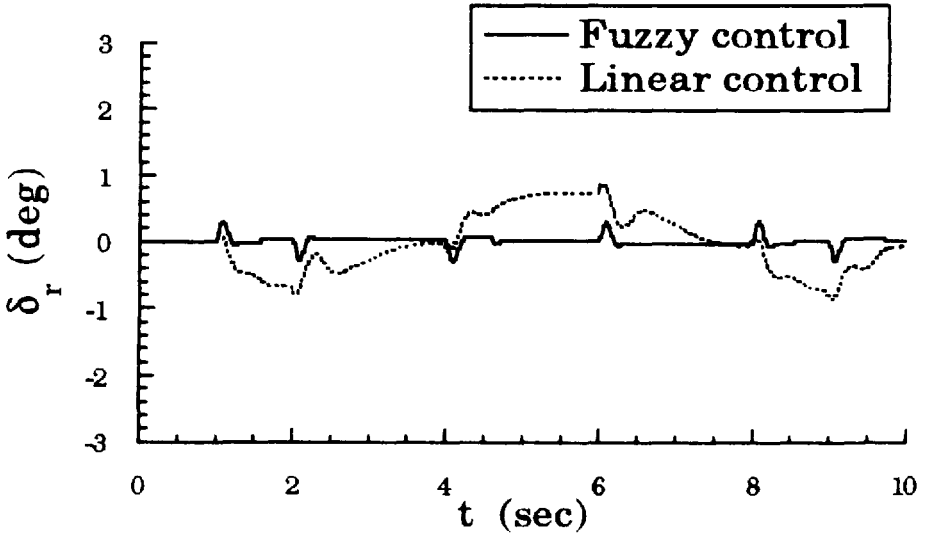

Figure 25 Rudder deflection at a 40° bank-to-bank command.

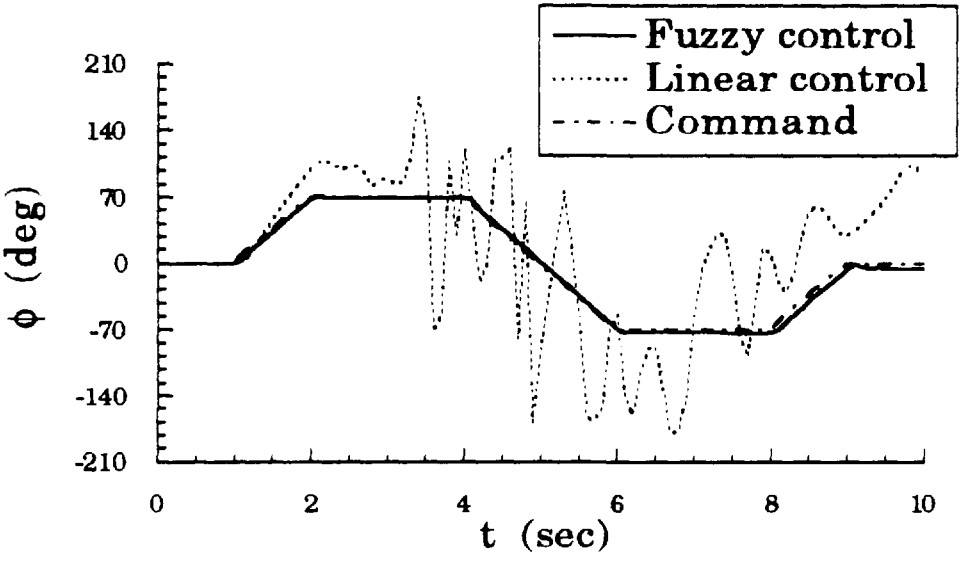

Figure 26 Bank angle at a 70° bank-to-bank command.

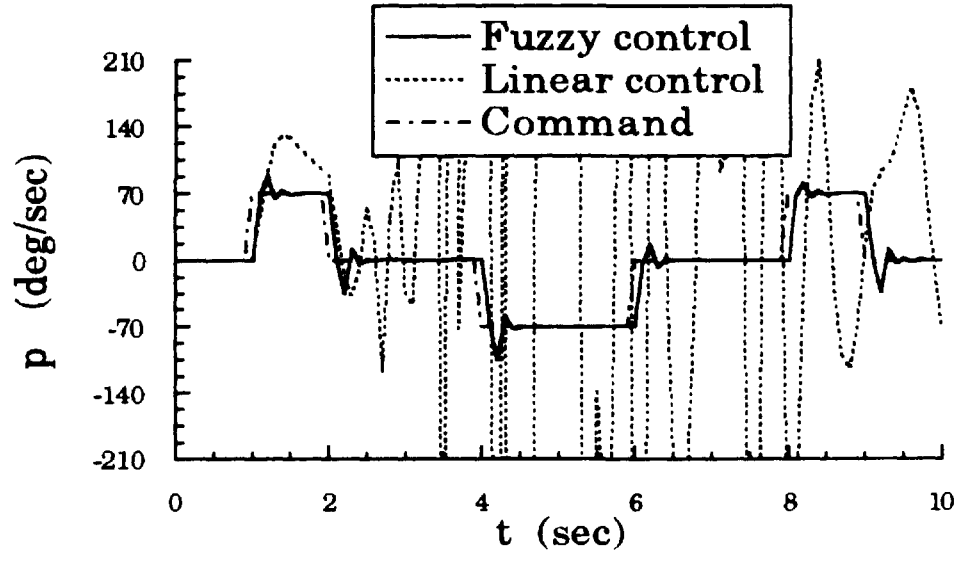

Figure 27 Roll rate at a 70° bank-to-bank command.